Erschienen in: 35th European Photovoltaic Solar Energy Conference and Exhibition / Verlinden, Pierre et al. (Hrsg.). - München : WIP, 2018. - S. 293-297. - ISBN 978-3-936338-50-8

INFLUENCE OF EMITTER LAYERS ON LETID KINETICS IN MULTICRYSTALLINE SILICON

Alona Otaegi[(1,2)], Daniel Skorka[(1)], Andreas Schmid[(1)], Annika Zuschlag[(1)], Juan Carlos Jimeno[(2)], and Giso Hahn[(1)]
[(1)]University of Konstanz, Department of Physics, 78457 Konstanz, Germany
[(2)]Technological Institute of Microelectronics, UPV/EHU, 48013 Bilbao, Spain

ABSTRACT: The influence of emitter layers on LeTID kinetics in multicrystalline silicon is analysed in this work. Multicrystalline silicon samples with emitter layers with sheet resistivity of 60, 175, 200, 230 and 360 Ω/sq have been processed and exposed afterwards to 1 sun illumination at 75ºC for more than 2000 h. The effective lifetime of the minority charge carriers of the samples has been measured repetitively by spatially resolved photoluminescence. The resulting lifetime maps are analysed and the effective defect concentration of the samples is calculated. This approach leads to different degradation rates, depending on the emitter sheet resistivity, and to the same defect regeneration rate, but differing in the onset of regeneration.
Keywords: Multicrystalline silicon; LeTID; degradation; regeneration; emitter layer

1 INTRODUCTION

The solar cell market is evolving towards a major implantation of PERC (passivated emitter and rear cell) cells over Al-BSF (back surface field) cells [1]. Efficiencies above 21% are obtained from PERC-type solar cells due to less recombination at the rear and the increase of rear surface reflection by an extra rear passivation [2-4], and production costs are close to standard Al-BSF technology [5]. However, this technology can be particularly sensitive to elevated temperatures under illumination in a phenomenon entitled LeTID (light and elevated temperature induced degradation), and the efficiency can drop by more than $10\%_{rel}$ [6-9].

The easiest way to describe the LeTID phenomenon in multicrystalline silicon (mc-Si) PERC solar cells is via a 3-state reaction scheme analogue to the effect observed for BO-degradation in Cz Si [10]; however, the inducing mechanisms are different for the different technologies, since BO complex formation and FeB pair dissociation have been found to be responsible for Cz Si degradation [11, 12], but have been discarded for LeTID [6-8].

While the main root causing LeTID remains unknown, changes in the processing steps are involved in the research for eliminating or reducing the effect. Gettering is shown to be efficient to diminish the degradation effect on good material quality [13]; a dark anneal after firing reduces LeTID [14]; exposing samples to elevated temperatures and high illumination accelerates the degradation and following regeneration process [15, 16]; and changing the temperature profile to avoid a fast cool cycle during firing avoids the effect [17, 18]. Up to now, most studies have shown the necessity to apply a thermal load after diffusion at temperatures well above 600°C (*e.g.* in form of a firing step) to activate the occurrence of LeTID (*e.g.* [19]). But latest results indicate that it is not the temperature load of the firing step that is needed, but the presence of hydrogen which is causing LeTID [20].

The relevance of the bulk lifetime and instabilities of the passivation layer have been subjects under study [21-24]; however, no mention of emitter layers and their influence on LeTID kinetics have been found in literature. This work aims to delve into a further characterization by analysing the influence of the presence of emitter layers on LeTID kinetics, which could help to understand the mechanisms involved.

2 EXPERIMENTAL DETAILS

Fig. 1 sketches the setup of the applied process sequence. Starting with 1.5 Ωcm boron doped mc-Si, wafers with comparable grain and defect structure (sister wafers) were used to study the influence of different emitter layers on LeTID.

The samples were chemically etched to remove saw damage. A standard gettering was applied afterwards by $POCl_3$ diffusion (60 Ω/sq). The emitter of some samples was then removed partially via wet chemical etch-back in order to analyse the influence of emitter layers' sheet resistivity R_{sheet} on the LeTID degradation and regeneration process. To avoid uncertainties of the etch-rate due to the different crystallographic orientations, R_{sheet} of the samples was measured on (100)-oriented Cz-samples. The measured R_{sheet} values correspond to 60 Ω/sq (no emitter removal), 175 Ω/sq, 200 Ω/sq, 230 Ω/sq and 360 Ω/sq (maximum emitter removal). A PECVD (plasma-enhanced chemical vapour deposition) SiN_x:H layer was then deposited on the samples and the manufacturing process was finished with a firing step in a belt furnace with peak wafer temperature of 786ºC, monitoring the temperature on the wafer surface with a K-type thermocouple.

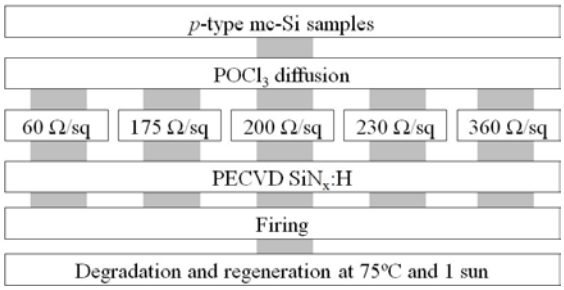

Figure 1: Process sequence of the investigated samples.

After firing, the samples are held at a temperature of approximately 75ºC on a hot-plate under constant illumination with halogen lamps (0.9±0.1 suns). Effective minority charge carrier lifetime τ_{eff} is measured repetitively by the fast and self-calibrated transient photoluminescence imaging (TR-PLI) method [25 26] at room temperature. For each measurement, a spatially resolved lifetime map is obtained, as well as the harmonic average τ_{eff}. This method allows tracking the changes in τ_{eff} in different areas of the samples

throughout the experiment.

3 RESULTS AND DISCUSSION

Fig. 2 shows τ_{eff} maps of three relevant stages throughout the experiment for the samples with R_{sheet} of 200 Ω/sq and 360 Ω/sq, respectively. The first stage corresponds to the initial situation, right after the firing with no degradation (left); the second stage corresponds to a full degradation of the samples with τ_{eff} below 20 µs after 400 h (middle). The third stage shows maps of the samples during regeneration (right).

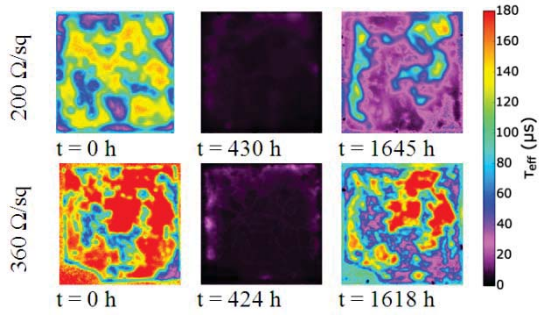

Figure 2: Effective lifetime mappings for samples with R_{sheet} of 200 Ω/sq (upper row) and 360 Ω/sq (lower row) directly after firing (left), around maximum degradation (middle) and after onset of regeneration (right).

Fig. 3 shows the evolution of the harmonic average τ_{eff} for all samples under study, from their initial state to above 2,000 h. In this figure, the initial τ_{eff} of the samples are different as expected, due to different recombination strengths in the emitter. Initially, the τ_{eff} distribution of all samples narrows down to a low lifetime level with different slopes. After around 100 h, the different samples show almost identical values indicating that the different emitter layers have no significant effect on maximum LeTID defect concentration. All the samples regenerate, although the onset of regeneration starts earlier for higher emitter sheet resistivities (inset in Fig. 3).

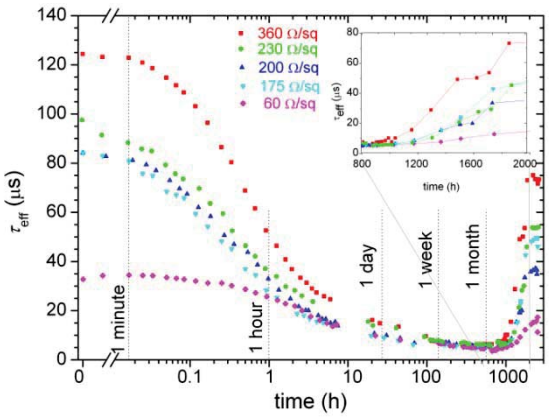

Figure 3: Evolution of the average τ_{eff} for the samples with different emitter layers (75°C, 0.9 suns).

The rainbow plot in Fig. 4 helps to recognize what is happening in each of the samples' regions; this rainbow plot represents the τ_{eff} behaviour during the experiment time for the sample. Each line in the graph represents an area of 150x150 µm^2 in the spatially resolved TR-PLI lifetime measurement and represents one of 2,500 small areas on the sample. The colour code applied is based on the initial $\tau_{eff}(0)$ of each sample at the beginning of the experiment. The dashed line represents the harmonic average τ_{eff} of the sample throughout the degradation-regeneration experiment. All investigated samples follow a similar tendency as shown exemplarily in Fig. 4 for the 200 Ω/sq sample. Regeneration sets in earlier in areas of high initial material quality (starting at 800 h in Fig. 4) and later in areas of lower initial material quality.

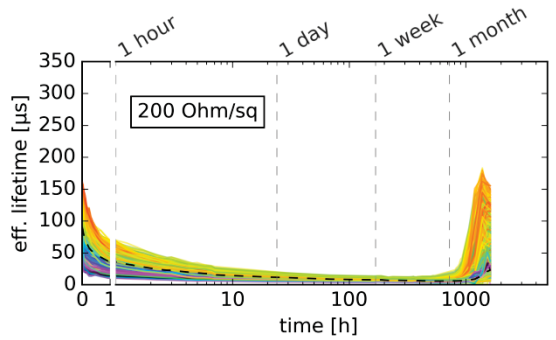

Figure 4: Effective lifetimes for a sample with emitter sheet resistivity of 200 Ω/sq (x-axis: 0-1 h linear scale, 1-2000 h log scale).

3.2 Analysis of the degradation

Degradation of the samples can be seen during the first few hundred hours of the experiment and all the samples show similar minimum average τ_{eff} values well below 10 µs after around 100 h of treatment time. However, two degradation behaviours can be detected from the data shown in Fig. 3; a *fast* degradation mechanism from the start of the experiment up to the first hour and a *slow* degradation mechanism from the first hour up to 100 h approximately. This evolution is consistent with [27].

To further quantify the degradation, the time-dependent effective defect concentration, $N^*(t)$, is determined as also used in, *e.g.*, [27-29].

(1)

For degradation, it is possible to fit $N^*(t)$ by a two exponential model as also used in [27]:

(2)

with a and b the pre-factors for the degradation rates R_{fast} and R_{slow}. Fig. 5 shows exemplarily the $N^*(t)$ values over treatment time for the two samples with 230 and 360 Ω/sq, respectively, using the fit parameters listed in Tab. I. The quality of the fits according to Eq. (2) (also included in Fig. 5 as solid lines) is generally very good and reliable as indicated by RMSE values close to 1. Nevertheless, fits to $N^*(t)$ using Eq. (2) for samples with 175 and 200 Ω/sq, respectively, resulted in slightly worse RMSE values, and fitting parameters obtained for these samples have a higher inaccuracy.

Table I shows the fitting parameters obtained with

MATLAB® for the pre-factors as well as for the degradation rates following the two exponential model.

Table I: Fitting of N^*(t) according to the two exponential model for the samples under study.

Emitter	Fast degradation		Slow degradation	
	a	R_{fast} [1/h]	*b*	R_{slow} [1/h]
60 Ω/sq	0.0589	0.150	0.132	0.00574
175 Ω/sq	0.0965	0.207	0.131	0.00364
200 Ω/sq	0.0836	0.181	0.115	0.00316
230 Ω/sq	0.0417	0.454	0.139	0.00717
360 Ω/sq	0.0251	0.534	0.129	0.0110

The fast degradation rate R_{fast} depends on the emitter sheet resistivity; in fact, the higher the R_{sheet}, the faster the degradation seems to happen; however, the slow degradation rate R_{slow} seems to be slightly less dependent on the characteristics of the emitter.

The two exponential model for degradation has already been reported for mc-Si material [19, 27].

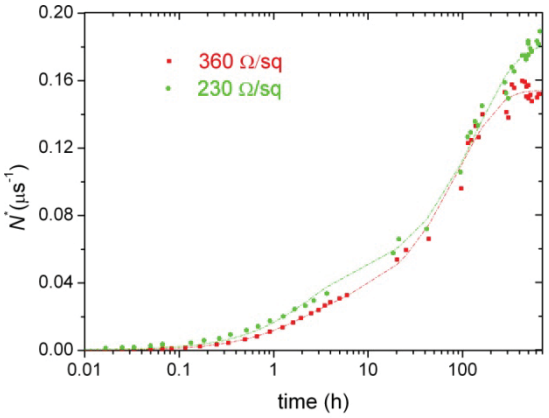

Figure 5: Evolution of N^* for the samples with R_{sheet} of 230 and 360 Ω/sq. The solid lines are numerically simulated by solving Eq. (2) using the coefficients from Tab. I.

3.3 Analysis of the regeneration

The inset of Fig. 3 shows the behaviour of the harmonic average τ_{eff} at the onset of regeneration for the samples under study, from 800 h up to the end. In this figure, it can be seen that regeneration of the samples starts around 1,000 h of treatment time.

The regeneration of the sample with maximum emitter removal (360 Ω/sq) begins earlier, and after >1,600 h the regeneration is more pronounced and areas with τ_{eff} of >180 μs can be found in regions far from the edge (from Fig. 2).

A more detailed sketch is shown in Fig. 6 where the evolution of N^* for all the samples is shown for the time interval of 800-2,500 h. In this figure, a fitting to a single exponential term is made for 60, 200 and 360 Ω/sq samples, shown with dash-dotted lines. According to the fitting, all the samples show the same regeneration rate, differing only in the moment at which regeneration starts. The higher the R_{sheet}, the earlier the regeneration starts. The three samples with R_{sheet} of 175, 200 and 230 Ω/sq show approximately the same N^* values over time.

The rainbow plot in Fig. 4 shows that even though the regions with the highest effective lifetime recover up to their initial value, regeneration is not complete as the average τ_{eff} is only around half of its initial value. This behaviour of incomplete regeneration has also been found in boron-oxygen defect experiments [30], where slow regeneration rates are related to incomplete regeneration processes. In addition, the SiN_x:H surface passivation degrades as well under these treatment conditions as shown, *e.g.*, in [23, 24].

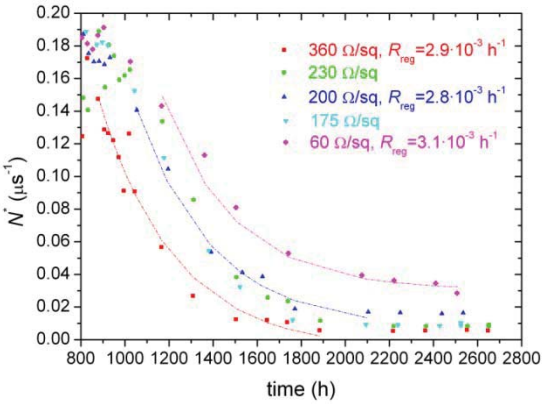

Figure 6: Evolution of N^*, from 800 h of experiment up to the end, for the samples under study.

It was speculated that regeneration rate is increased by higher excess carrier density Δn (*e.g.*, [8, 13]), but in our case Δn should be almost identical for all samples between 100-900 h of treatment. Nevertheless, the samples with lower emitter sheet resistivity show an earlier onset of regeneration leaving room for other explanations.

4 CONCLUSIONS

The influence of the emitter layers on LeTID kinetics in mc-Si was analysed in this work. The LeTID effect for samples with emitter sheet resistivities of 60, 175, 200, 230, and 360 Ω/sq, respectively, was studied at 75ºC and 1 sun illumination for more than 2,000 h. The evolution of the samples was tracked via lifetime maps obtained by TR-PLI measurements.

In terms of degradation, two behaviours have been observed; a fast degradation rate, relevant up to the first hour approximately, and a slow degradation rate, from 1 hour up to 100 hours. The fast degradation rate seems to be dependent on the emitter nature, and is faster for higher emitter sheet resistivities. The slow degradation rate does not seem to be influenced by the nature of the emitter.

In terms of regeneration, similar regeneration rates have been found regardless of the emitter sheet resistivity, but the regeneration starts earlier for higher emitter sheet resistivities, although harmonic average τ_{eff} values are almost identical at maximum degradation in all samples. None of the samples is fully regenerated after ~1,800 h of treatment and the harmonic average τ_{eff} remains at about half its initial value. The regeneration seems to be better (more complete) in good quality material areas of the samples.

5 ACKNOWLEDGEMENTS

Alona Otaegi would like to gratefully acknowledge the entire team of the Department of Physics in the University of Konstanz for the assistance received during her postdoctoral stay, and especially K. Bayer, J. Lindroos, K. Weller, J. Fichtner, L. Mahlstädt, B. Rettenmaier, A. Dastgheib-Shirazi, and J. Engelhart for technical assistance.

This research has been supported by the Secretary of State for Research, Development and Innovation, attached to the Spanish Ministry of the Economy and Competitiveness, in its project TABACO ENE2014-56069-CA. Part of this work was supported by the German BMWi under contract numbers 0325763B, 0324204B, and 0324001. The content is the responsibility of the authors.

6 REFERENCES

[1] International Technology Roadmap for Photovoltaic (ITPV): Results 2017, ninth edition. July 2018. See http://www.itrpv.net/Reports/Downloads/

[2] A. W. Blakers, A. Wang, A. M. Milne, J. Zhao, and M. A. Green, "22.8% efficient silicon solar cell", Appl. Phys. Lett. vol. 55, pp. 1363-1365, 1989.

[3] M. A. Green, "The passivated emitter and rear cell (PERC): from conception to mass production", Sol. Energy Mater. Sol. Cells, vol. 143, pp. 190-197, 2015.

[4] O. Schultz, S. W. Glunz, and G. P. Willeke, "Multicrystalline silicon solar cells exceeding 20% efficiency", Prog. Photovolt: Res. Appl., vol. 12, pp. 553-558, 2004.

[5] P. A. Basore, "Understanding manufacturing cost influence on future trends in silicon photovoltaics", IEEE J. Photovolt., vol. 4, No. 6, pp. 1477-1492, 2014.

[6] K. Ramspeck, S. Zimmermann, H. Nagel, A. Metz, Y. Gassenbauer, B. Birkmann, and A. Seidl, "Light induced degradation of rear passivated mc-Si solar cells" Proc. of the 27th EU PVSEC, pp. 861-865, 2012.

[7] F. Fertig, K. Krauß, I. Geisemeyer, J. Broisch, H. Höffler, and J. Ove Odden, "Fully solderable large-area screen-printed Al-BSF p-type mc-Si solar cells from 100% solar grade feedstock yielding $\eta > 17\%$: challenges and potential on cell and module level", Proc. of the 27th EU PVSEC, pp. 1031-1038, 2012.

[8] F. Kersten, P. Engelhart, H. -C. Ploigt, A. Stelnikov, T. Lindner, F. Stenzel, M. Bartzsch, A. Szpeth, K. Petter, J. Heitmann, and J. W. Müller, "Degradation of multicrystalline silicon solar cells and modules after illumination at elevated", Sol. Energy Mater. Sol. Cells, vol. 142, pp. 83-86, 2015.

[9] F. Kersten, F. Fertig, K. Petter, B. Klöter, E. Herzog, M. B. Strobel, J. Heitmann, and J. W. Müller, "System performance loss due to LeTID", Energy Procedia, vol. 124, pp. 540–546, 2017.

[10] A. Herguth, G. Schubert, M. Kaes, and G. Hahn, "Investigations on the long time behavior of the metastable boron-oxygen complex in crystalline silicon", Progr. Photovolt. Res. Appl., vol. 16, pp. 135-140, 2008.

[11] J. Schmidt, A. G. Aberle, and R. Hezel, "Investigation of carrier lifetime instabilities in Cz-grown silicon", Proc. 26th IEEE PVSC, pp. 13-19, 1997.

[12] L. J. Geerligs, and D. Macdonald, "Dynamics of light-induced FeB pair dissociation in crystalline silicon", Appl. Phys. Lett., vol. 85, 5227, 2004.

[13] A. Zuschlag, D. Skorka, and G. Hahn, "Degradation and regeneration analysis in mc-Si after different gettering steps", Prog. Photovolt: Res. Appl., vol. 25, pp. 545-552, 2017.

[14] C. Chan, T. H. Fung, M. Abbott, D. Payne, A. Wenham, B. Hallam, R. Chen, and S. Wenham, "Modulation of carrier-induced defect kinetics in multi-crystalline silicon PERC cells through dark annealing", Sol. RRL, 1600028, 2017.

[15] K. Krauβ, A. A. Brand, F. Fertig, S. Rein, and J. Nekarda, "Fast regeneration processes to avoid light-induced degradation in multicrystalline silicon solar cells", IEEE J. Photovolt., vol. 6, No. 6, pp. 1427-1431, 2016.

[16] D. N. R. Payne, C. E. Chan, B. J. Hallam, B. Hoex, M. D. Abbott, S. R. Wenham, and D. M. Bagnall, "Rapid passivation of carrier-induced defects in p-type multi-crystalline silicon", Sol. Energ. Mat. Sol. Cells, vol. 158, pp. 102-106, 2016.

[17] R. Eberle, W. Kwapil, F. Schindler, S. W. Glunz, and M. C. Schubert, "Firing temperature profile on light induced degradation of multicrystalline silicon", Phys. Status Solidi RRL, vol. 10, pp. 861–865, 2016.

[18] R. Sharma, A. G. Aberle, and J. B. Li, "Optimization of belt furnace anneal to reduce light and elevated temperature induced degradation of effective carrier lifetime of p-type multicrystalline silicon wafers," Sol. RRL vol. 2, 1800070, 2018.

[19] D. Bredemeier, D. Walter, S. Herlufsen, and J. Schmidt, "Lifetime degradation and regeneration in multicrystalline silicon under illumination at elevated temperature", AIP Advances, vol. 6, 035119, 2016.

[20] M.A. Jensen, A. Zuschlag, D. Skorka, S. Wieghold, A.E. Morishige, G. Hahn, T. Buonassisi, "Evaluating root cause: the distinct roles of hydrogen and firing in activating light- and elevated-temperature induced degradation", J. Appl. Phys., vol. 124(8), 085701, 2018.

[21] A. Zuschlag, D. Skorka, and G. Hahn, "Degradation and regeneration analysis in mc-Si", Proc. 43rd IEEE PVSC, pp. 1051-1054, 2016.

[22] F. Kersten, J. Heitmann, and J. W. Müller, "Influence of Al_2O_3 and SiN_x passivation layers on LeTID", Energy Procedia, vol. 92, pp. 828-832, 2016.

[23] D. Sperber, A. Herguth, and G. Hahn, "Instability of dielectric surface passivation quality at elevated temperature and illumination", Energy Procedia, vol. 92, pp. 211-217, 2016.

[24] D. Sperber, A. Heilemann, A. Herguth, and G. Hahn, "Temperature and light induced changes in bulk and passivation quality of boron-doped float-zone silicon coated with SiN_x:H", IEEE J. Photovolt., vol. 7, No. 2, pp. 463-470, 2017.

[25] D. Kiliani, G. Micard, B. Steuer, B. Raabe, A. Herguth, and G. Hahn, "Minority charge carrier lifetime mapping of crystalline silicon wafers by time-resolved photoluminescence imaging," J. Appl. Phys., vol. 110, 054508, 2011.

[26] D. Kiliani, A. Herguth, G. Micard, J. Ebser, and G. Hahn, "Time-resolved photoluminescence imaging with electronic shuttering using an image intensifier unit", Sol. Energ. Mat. Sol. Cells, vol. 106, pp. 55-59, 2012.

[27] D. Bredemeier, D. Walter, and J. Schmidt, "Light-induced lifetime degradation in high-performance multicrystalline silicon: detailed kinetics of the defect activation", Sol. Energ. Mat. Sol. Cells, vol. 173, pp. 2-5, 2017.

[28] J. Lindroos, and H. Savin, “Review of light-induced degradation in crystalline silicon solar cells”, Sol. Energ. Mat. Sol. Cells, vol. 147, pp. 115-126, 2016.
[29] M. A. Jensen, A. E. Morishige, J. Hofstetter, D. B. Needleman, S. Chakraborty, R. Sharma, H. S. Laine, B. Lai, V. Rose, A. Youssef, E. E. Looney, S. Wieghold, J. R. Poindexter, J. E. Correa-Baena, T. Felisca, H. Savin, J. B. Li, and T. Buonassisi, “Solubility and diffusivity: important metrics in the search of the root cause of light- and elevated temperature-induced degradation”, IEEE J. Photovolt., vol. 8, No. 2, pp. 448-455, 2018.
[30] S. Wilking, M. Forster, A. Herguth, and G. Hahn, “From simulation to experiment: understanding BO-regeneration kinetics”, Sol. Energ. Mat. Sol. Cells, vol. 142, pp. 87-91, 2015.